Magnetic and magnetoelectric study of the pyroxene $NaCrSi_2O_6$

Gwilherm Nénert,[1,*] Ingyu Kim,[2] Masahiko Isobe,[3] Clemens Ritter,[1] Alexander N. Vasiliev,[4] Kee Hoon Kim,[2] and Yutaka Ueda[3]

[1]*Institut Laue-Langevin, Boîte Postale 156, 38042 Grenoble Cedex 9, France*

[2]*CeNSCMR, Department of Physics and Astronomy, Seoul National University, Seoul 151-747, Korea*

[3]*Institute for Solid State Physics, University of Tokyo, 5-1-5 Kashiwa, Chiba 277-8581, Japan*

[4]*Low Temperature Physics Department, Moscow State University, Moscow 119991, Russia*

(Received 29 January 2010; revised manuscript received 16 April 2010; published 7 May 2010)

We investigated the magnetic, magnetoelectric, and crystal structures of the pyroxene $NaCrSi_2O_6$ by superconducting quantum interference device (SQUID) magnetometry, electrical polarization measurement, and powder neutron diffraction. Magnetic exchange couplings extracted from magnetization measurements are found to be $J_{intra}/k_b=-0.48(4)$ K and $J_{inter}/k_b=0.24(8)$ K. This is in perfect agreement with the antiferromagnetic order determined below $T_N=2.8(2)$ K by neutron diffraction. Corroborating the determined magnetic structure (magnetic symmetry C-1′), the magnetic field dependence of electrical polarization evidences a clear magnetoelectric effect below T_N. An induced magnetic field transition toward a ferromagnetic state (magnetic symmetry C2′/c′) is observed in the SQUID data and confirmed by neutron diffraction.

DOI: 10.1103/PhysRevB.81.184408 PACS number(s): 75.85.+t, 75.10.Pq, 91.60.Pn, 75.25.−j

I. INTRODUCTION

In recent years, the coupling between magnetic and dielectric properties in transition-metal oxides gave rise to a significant research effort.[1–3] This effort is governed by the emergence of new fundamental physics and potential technological applications.[2–4] Multiferroic materials exhibit simultaneously (ferro)magnetic, pyroelectric, and ferroelastic properties. Contrary to multiferroic materials, magnetoelectric materials show an induced electrical polarization by a magnetic field. A proper understanding of the interplay between the various physical properties of these two types of materials relies heavily on the knowledge of the detailed crystal and magnetic structures.

Lately, three materials ($NaFeSi_2O_6$, $LiFeSi_2O_6$, and $LiCrSi_2O_6$) belonging to the pyroxene family have been reported as multiferroic materials. It has been shown that $LiCrSi_2O_6$ and $LiFeSi_2O_6$ are, in fact, magnetoelectric materials rather than multiferroics.[5,6]

Jodlauk *et al.*[7] suggested that several members of the pyroxene family should have an incommensurate magnetic structure. This suggestion was based on some theoretical assumptions and linked to the geometrical magnetic frustration present in this family.[7,8] However, for the moment it turned out that most of the pyroxenes exhibit a simple magnetic structure commensurate with the lattice with $\mathbf{k}=0$.[5,6,9–12] Nevertheless, several of those reported magnetic structures are compatible with a linear magnetoelectric effect.[5,6,9,11]

In this contribution, we continue our investigation of the crystal and magnetic structures of the pyroxene family by studying $NaCrSi_2O_6$. We have investigated its magnetic properties using superconducting quantum interference device (SQUID) magnetometry and powder neutron diffraction as function of temperature and magnetic field. We show that $NaCrSi_2O_6$ contrary to $NaCrGe_2O_6$ exhibits an antiferromagnetic ground state characterized by a commensurate magnetic structure defined by $\mathbf{k}=0$. Contrary to Li containing pyroxenes like $LiMSi_2O_6$ (M=V,Cr,Fe) (Refs. 5, 9, and 10) the magnetic structure is described by the direct product of two irreducible representations. The associated magnetic symmetry is C-1′ and allows a linear magnetoelectric effect.[13] In agreement with the determined magnetic structure, the magnetic field dependence of the electrical polarization evidences a clear magnetoelectric effect. We find that the magnetic moment of Cr^{3+} is equal to $2.31(4)\mu_B$ at 1.8 K. Magnetic-susceptibility data are well described by a pseudo-one-dimensional Heisenberg chain of $S=3/2$ spins giving rise to an antiferromagnetic intrachain magnetic exchange coupling and a ferromagnetic interchain magnetic exchange coupling. Powder neutron diffraction at low temperature confirms the existence of both antiferromagnetic and ferromagnetic exchange interactions. The magnetic structure is described by ferromagnetic layers coupled antiferromagnetically while moving along the c axis. Applying magnetic field, a transition to a ferromagnetic phase characterized by the space group C2′/c′ is induced. This field-induced magnetic symmetry is identical to the one reported for the zero-field magnetic structure of $NaCrGe_2O_6$.[12]

II. EXPERIMENT

Polycrystalline samples of $NaCrSi_2O_6$ were prepared by a solid-state reaction with an appropriate molar ratio of Na_2CO_3, Cr_2O_3, and SiO_2. The weighted mixtures were pressed into pellets and heated at 1273 K in air for several days with one intermediate grinding.

Neutron-diffraction measurements were carried out on powder of $NaCrSi_2O_6$. The precise crystal and magnetic structures were investigated using high-resolution powder data at room temperature, 10 and 1.8 K using the D2B diffractometer at the ILL. The measurements were carried out at a wavelength of 1.594 Å corresponding to the (335) Bragg reflection of a germanium monochromator. The neutron detection is performed with ^{3}He counting tubes spaced at 1.25° intervals. A complete diffraction pattern is obtained after 25 steps of 0.05° in 2θ. Additional neutron-diffraction measure-

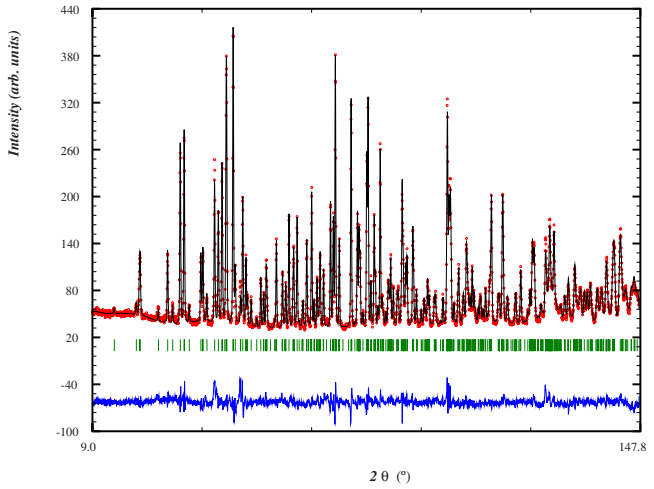

FIG. 1. (Color online) The neutron pattern (λ=1.594 Å) of $NaCrSi_2O_6$ sample collected at 10 K using the D2B diffractometer. The refinement has been done in the C2/c space group with a =9.5644(5) Å, b=8.6985(5) Å, c=5.2635(3) Å, and β =107.5076(9)° with the following statistics: R_p=4.85% and R_{wp} =6.37%.

ments have also been recorded on $NaCrSi_2O_6$ samples in magnetic fields up to 6 T at 1.8 K using a cryomagnet. The powder was pressed in tablets in order to preclude the grains from reorientating in the magnetic field. Diffraction-data analysis was done using the FULLPROF refinement package.[14]

In order to measure magnetoelectric (ME) current, the $NaCrSi_2O_6$ pellet was thinned down to 0.315 mm in thickness. Silver epoxy was used to make electrodes on both sides of the pellet. In general, both magnetic field and electric field can be applied for the ME cooling process. However, in our case, we found that application of electric field to our rather leaky polycrystalline specimen from high temperatures resulted in large background current during the ME-current measurement. This comes mainly from the so-called space charges trapped inside the polycrystalline specimen. Thus, to reduce such space charges, we cooled down the sample from 5 to 2 K under H=9 or −9 T without electric field, and applied E=317 kV/m at 2 K and swept the magnetic field at a ramping rate of 200 Oe/s from 9 (−9 T) to −9 (9 T) under the same electric field. The ME current was measured with Keithley 617 electrometer. After subtraction of the small constant value of current at a starting magnetic field, we integrate the ME current to get the change in the electrical polarization P [$\Delta P = P - P(9\ \mathrm{T})$].

III. RESULTS

A. Crystal structure

The crystal structure of $NaCrSi_2O_6$ was investigated at 1.8, 10, and 300 K by powder neutron diffraction. All patterns were refined in the space group C2/c, taking the structure reported by Origlieri *et al.*[15] as a starting structural model. The refined lattice parameters are a=9.5644(5) Å, b=8.6985(5) Å, c=5.2635(3) Å, and β=107.5076(9)° at 10 K. Our refinement at room temperature is similar to the single-crystal study reported previously.[15] Since the crystal structure of the pyroxene family has been investigated in details already in the literature,[10,15–17] we shall present here only our results at 10 K. The good agreement between the calculated and observed neutron powder patterns at 10 K is presented in Fig. 1. The refined atomic coordinates are presented in Table I.

B. SQUID measurements

The temperature dependencies of the magnetic susceptibility were measured in external magnetic fields of 50 and 1000 Oe. The low magnetic field measurement shown in Fig. 2 displays a broad maximum at 3.6 K which is a signature of the low dimension of the system. Only the derivative $d\chi/dT$ can give an exact indication of the magnetic ordering temperature. We observe that $d\chi/dT$ presents a maximum at 2.8(2) K, which we interpret as the antiferromagnetic ordering temperature, in agreement with previous specific-heat data.[18] We fitted the magnetic susceptibility with a Curie-Weiss temperature dependence defined by $\chi = \frac{C}{T-\theta}$. The fit was made in the range 100–350 K. We see that the magnetic susceptibility departs from the Curie-Weiss model below 30–35 K. The determined effective moment amounts to μ_{eff}=3.432(1)μ_B while θ=−0.22(8) K. This is in agreement with a previous report.[18] The field dependence of the magnetization is presented in Fig. 3. The saturation value is about 2.56μ_B in a magnetic field of 7×10^4 Oe. However, we notice that the magnetization is not fully saturated at the maximum applied field. The derivative dM/dT is presented in Fig. 3(b) and evidences a field-induced phase transition for $H > 3.1(1)\times10^4$ Oe at 2 K.

TABLE I. Crystallographic coordinates extracted from the Rietveld refinement carried out on powder neutron diffraction (D2B) using the space group C2/c at 10 K with a=9.5644(5) Å, b=8.6985(5) Å, c =5.2635(3) Å, and β=107.5076(9)°.

Atom	Wyckoff	x	y	z	U_{iso}
Na	4e	0	0.3008(4)	0.25	0.0070(8)
Cr	4e	0	0.9084(4)	0.25	0.0049(7)
Si	8f	0.2928(2)	0.0923(2)	0.2340(4)	0.0024(4)
O_1	8f	0.11419(15)	0.07933(18)	0.1374(3)	0.0036(3)
O_2	8f	0.36058(18)	0.25953(17)	0.3053(3)	0.0039(3)
O_3	8f	0.35395(17)	0.01048(16)	0.0095(3)	0.0037(3)

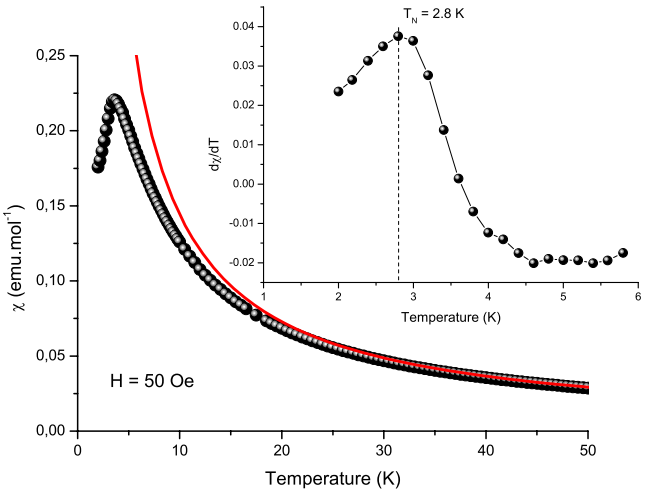

FIG. 2. (Color online) Magnetic susceptibility measured on a $NaCrSi_2O_6$ powder sample with $H=50$ Oe. The inset shows the derivative $d\chi/dT$ which gives evidence for an antiferromagnetic order below $T_N=2.8(2)$ K. The line represents a Curie-Weiss temperature dependence fit between 100 and 300 K defined by $\chi=\frac{C}{T-\theta}$.

One characteristic of these pyroxene materials is that they are good representatives of low-dimensional magnetism with linear chains running along the c axis.[12,18] Consequently one can try to treat the magnetic-susceptibility data using low-dimensional magnetism formula.[19]

For a uniform chain of classical spins based on the Hamiltonian $\mathcal{H}=-2J\Sigma_i\mathbf{S}_i\mathbf{S}_{i+1}-g\mu_B[S(S+1)]^{1/2}-\Sigma_i\mathbf{H}\cdot S_i$, the magnetic susceptibility can be expressed as[19]

$$\chi_{chain}=\frac{Ng^2\beta^2S(S+1)}{3k_bT}\times\frac{1+u}{1-u}, \tag{1}$$

where u is the well-known Langevin function defined as $u=\coth[2JS(S+1)/k_bT]-k_bT/[2JS(S+1)]$ with $S=3/2$. Considering the three-dimensional ordering at 2.8(2) K, we assumed an interchain interaction J' between the antiferromagnetic chains. Applying the mean-field approximation,[20] the susceptibility of $NaCrSi_2O_6$ can be expressed as

$$\chi=\frac{\chi_{chain}}{1-\left(\frac{zJ'}{Ng^2\beta^2}\right)\chi_{chain}}, \tag{2}$$

where z is the number of nearest-neighbor chains, N Avogadro's number, g the gyromagnetic factor of a free-electron spin, and β the Bohr magneton. With g fixed at 2.00, the least-squares fit of the experimental data above 15 K to the above expression led to $J/k_b=-0.48(4)$ K, a Curie constant $C=1.4894(9)$ emu mol^{-1} K^{-1} (spin-only value, $C=1.875$ emu mol^{-1} K^{-1}) corresponding to $\mu_{eff}=3.452(1)\mu_B$ (spin-only value, $\mu_{theo}=3.873\mu_B$) and an interchain exchange coupling $J'/k_b=0.24(8)$ K taking into account $z=4$. The resulting fit is shown together with the experimental data in Fig. 4.

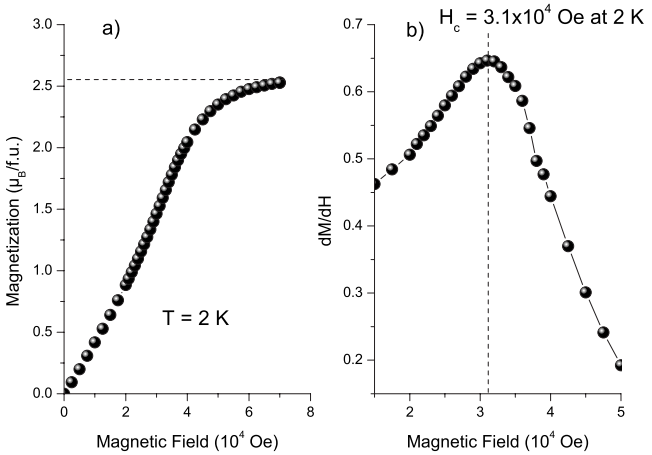

FIG. 3. (a) Magnetic field dependence of the magnetization measured on a $NaCrSi_2O_6$ powder sample at 2 K. (b) Derivative dM/dH at 2 K exhibiting the field-induced phase transition for $H_c=3.1(1)\times10^4$ Oe.

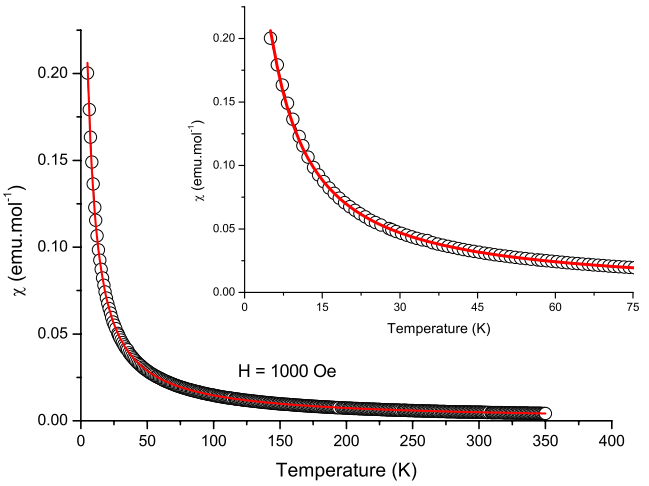

FIG. 4. (Color online) Temperature dependence of the magnetic susceptibility χ with $H=1000$ Oe. The solid line represents the best fit of the experimental data to Eq. (2) for $T>15$ K.

The result of the fit of Eq. (2) suggests that the coupling between the CrO_6 chains is ferromagnetic while the coupling within the chains is antiferromagnetic. We will see in Sec. III C that this is effectively the case.

C. Magnetic structure in zero magnetic field

In the powder pattern recorded at 1.8 K, several peaks appear while others increase in intensity compared to the data collected at 10 K. These peaks can be all indexed on the basis of the chemical cell and thus $\mathbf{k}=0$.

The possible magnetic structures compatible with the symmetry of $NaCrSi_2O_6$ and a magnetic propagation vector $\mathbf{k}=0$ have been discussed previously.[12] Keeping the same notations, we recall here the results of the derivations in Tables II and III.

According to the SQUID results, $NaCrSi_2O_6$ orders antiferromagnetically without detectable ferromagnetic moment. Consequently, one has *a priori* two possibilities for the antiferromagnetic structure according to Table III: either the magnetic structure associated to the IR Γ_2 ($L_y\neq0$), or the

TABLE II. Irreducible representations of the space group C2/c for $\mathbf{k}=0$. The symmetry elements are written according to Kovalev's notation, Ref. 21, $\tau=(0,0,\frac{1}{2})$.

	h_1	$h_3/(\tau)$	$h_{25}/(\tau)$	$h_{27}/(\tau)$
Γ_1	1	1	1	1
Γ_2	1	1	−1	−1
Γ_3	1	−1	1	−1
Γ_4	1	−1	−1	1

magnetic structure associated to the IR Γ_4 ($L_x \neq 0$ and $L_z \neq 0$).

We have performed refinements using both two models and present the results in Figs. 5 and 6. The associated R_{mag}'s are 18.05% and 15.43%, respectively, for the models associated to the IRs Γ_2 and Γ_4. Although the model using the IR Γ_4 is better than the one using the IR Γ_2, this model does not describe properly the magnetic intensity of the reflections (110) and $(1\bar{1}0)$ ($2\theta=14.55°$). Consequently one needs to consider other possible magnetic structures.

While most of the magnetic structures can be described by only one IR which corresponds to a Hamiltonian developed to the second order, it can be sometimes necessary to use more than one IR.[22] In that case, one has to consider the possible direct products between the various active IRs. The only possible direct product between two IRs, which does not give rise to a possible ferromagnetic component, is in our case the direct product between the two IRs giving rise to an antiferromagnetic structure: $\Gamma_2 \times \Gamma_4$ (see Table IV). The magnetic structure associated to this direct product gives rise to the following coupling:

$$\vec{M}(\mathrm{Cr}_1):(L_x,L_y,L_z),$$

$$\vec{M}(\mathrm{Cr}_2):(L_x,L_y,L_z),$$

$$\vec{M}(\mathrm{Cr}_3):(-L_x,-L_y,-L_z),$$

$$\vec{M}(\mathrm{Cr}_4):(-L_x,-L_y,-L_z). \quad (3)$$

The refinement using the magnetic structure model resulting from the direct product $\Gamma_2 \times \Gamma_4$ describes much better all the magnetic reflections and in particular the reflection at $2\theta=14.55°$. We find that experimentally $L_x=0$ within the resolution of our data, $L_y=1.50(6)\mu_B$ and $L_z=1.75(6)\mu_B$. The

TABLE III. Basis vectors for the atoms of the 4*e* site.

Basis vectors	*x*	*y*	*z*
Γ_1		M_y	
Γ_2		L_y	
Γ_3	M_x		M_z
Γ_4	L_x		L_z

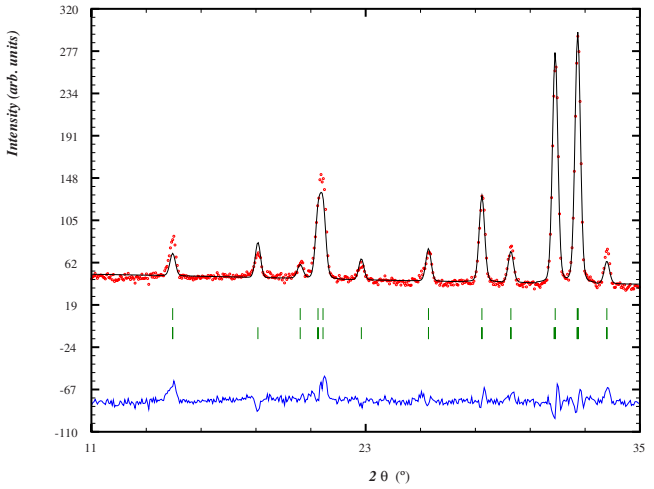

FIG. 5. (Color online) Refinement carried out using the magnetic structure associated to the IR Γ_2 at 1.8 K.

corresponding R_{mag} is 10.3% and the resulting fit is presented in Fig. 7. At 1.8 K, the magnetic moment of Cr^{3+} is $\|\mu(Cr^{3+})\|=2.31(4)\mu_B$.

The magnetic structure of $NaCrSi_2O_6$ at 1.8 K can be described by ferromagnetic layers alternating along the *c* axis resulting in a global antiferromagnetic order. A representation of the magnetic structure is illustrated in Fig. 8. This magnetic structure is in perfect agreement with the determined values for the magnetic exchange coupling constants from the magnetization data.

D. Study of the magnetic field dependence

The magnetic-susceptibility data show that there is a field-induced magnetic phase in $NaCrSi_2O_6$ (see Fig. 3) at 2 K, the critical field is $H_c=3.1(1)\times 10^4$ Oe. Consequently we have investigated the magnetic field dependence of the magnetic structure using neutron diffraction.

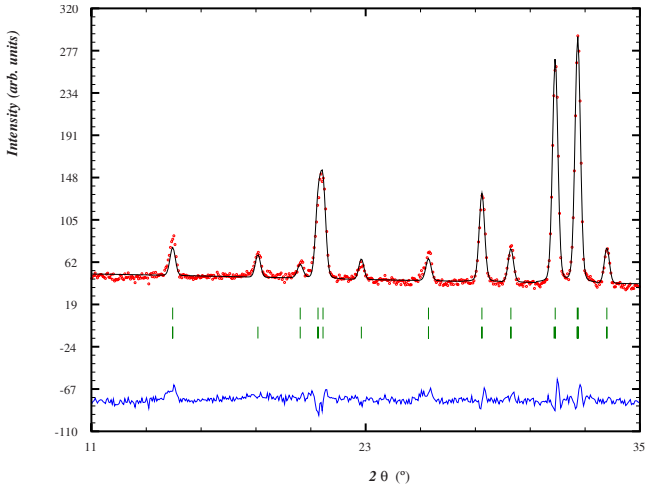

FIG. 6. (Color online) Refinement carried out using the magnetic structure associated to the irreducible representation Γ_4 at 1.8 K.

TABLE IV. Characters associated to the irreducible representations Γ_2, Γ_4 and their direct product. The symmetry elements are written according to Kovalev's notation, Ref. 21, $\tau=(0,0,\frac{1}{2})$.

	h_1	$h_3/(\tau)$	$h_{25}/(\tau)$	$h_{27}/(\tau)$
Γ_2	1	1	−1	−1
Γ_4	1	−1	−1	1
$\Gamma_2\times\Gamma_4$	1	−1	1	−1

The neutron powder diffraction patterns collected as function of magnetic field at 1.8 K on the D2B diffractometer are shown in Fig. 9. The field dependence shows that while the intensity of the reflections $(1\bar{1}0)$, (110), and (200) increases, the intensity of the reflection (001) decreases and finally vanishes at 6 T. All the magnetic reflections can still be indexed with the propagation vector $\mathbf{k}=0$ as in the zero-field magnetic structure.

We have carried out refinements of the $H=6$ T data with various models according to Table II. The best fit of the magnetic structure at $H=6$ T is given by the ferromagnetic spin arrangement described by the IR Γ_3. The field-induced magnetic transition at 1.8 K corresponds to a transition from an antiferromagnetic ground state C-1′ toward a ferromagnetic symmetry C2′/c′ with $M_x=-1.4(1)\mu_B$ and $M_z=1.81(7)\mu_B$. We present this final refined pattern measured at 1.8 K under $H=6$ T in Figs. 10 and 11 the associated ferromagnetic structure.

IV. MAGNETOELECTRIC COUPLING

The magnetic structure determined from neutron diffraction at zero field allows for the presence of a linear magnetoelectric effect. Revealing the actual presence of this possible linear magnetoelectric effect in $NaCrSi_2O_6$ would further confirm the interest that presents the pyroxene family

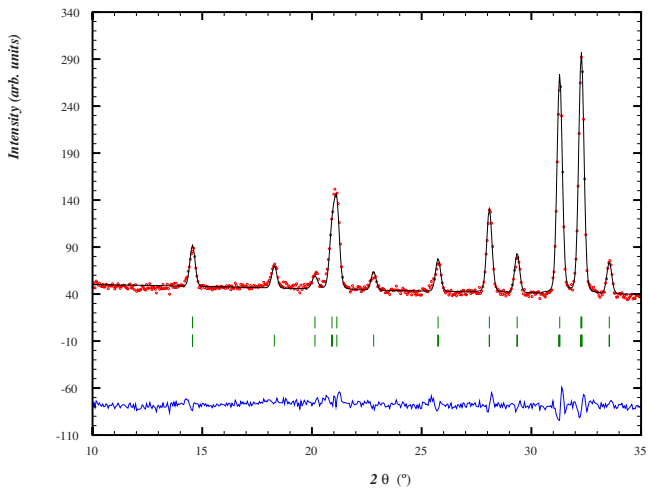

FIG. 7. (Color online) The neutron pattern (λ=1.594 Å) of $NaCrSi_2O_6$ sample collected at 1.8 K and $H=0$ T using the D2B diffractometer refined with an antiferromagnetic moment $\mu(Cr^{3+})=[0,1.50(6),1.75(6)]$.

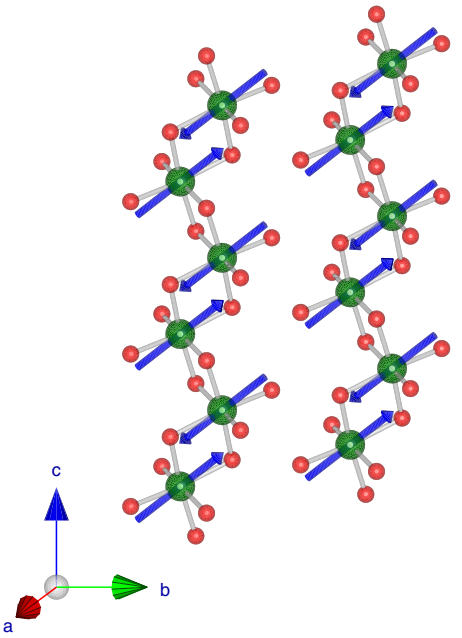

FIG. 8. (Color online) Magnetic structure of $NaCrSi_2O_6$ at 1.8 K and $H=0$ T described by $\Gamma_2\times\Gamma_4$. The magnetic coupling between the chains is ferromagnetic forming ferromagnetic layers alternating antiferromagnetically along the c axis. The magnetic structure representation has been made using VESTA (Ref. 23).

to find new magnetoelectric and/or multiferroic materials.

In order to observe the magnetoelectric effect, we have cooled down the sample from 5 to 2 K in an applied magnetic field of 9 T and the ME current was measured under a constant electric field of 317 kV/m while sweeping the magnetic field from 9 to −9 T to 9 T at a rate of 200 Oe/s. We present our results in Fig. 12. It can be clearly observed, a linear dependence of the induced electrical polarization is up to a magnetic field of around 3 T. Above this magnetic field,

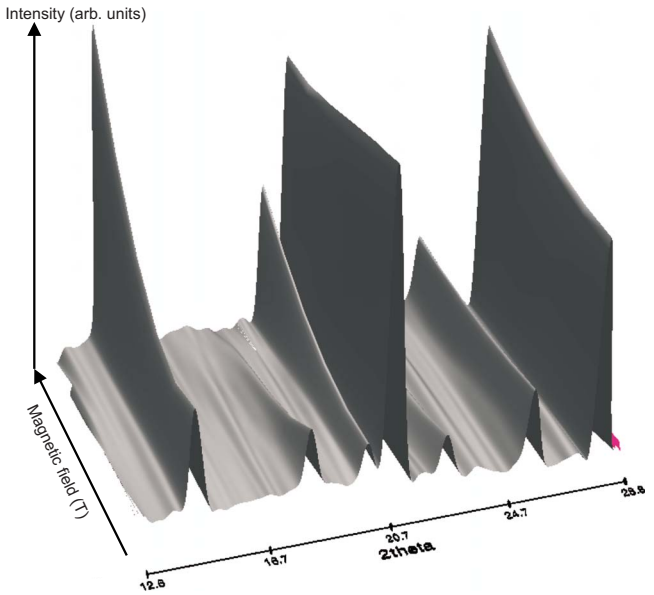

FIG. 9. (Color online) Field dependence of the diffraction pattern of $NaCrSi_2O_6$ recorded on D2B at 1.8 K.

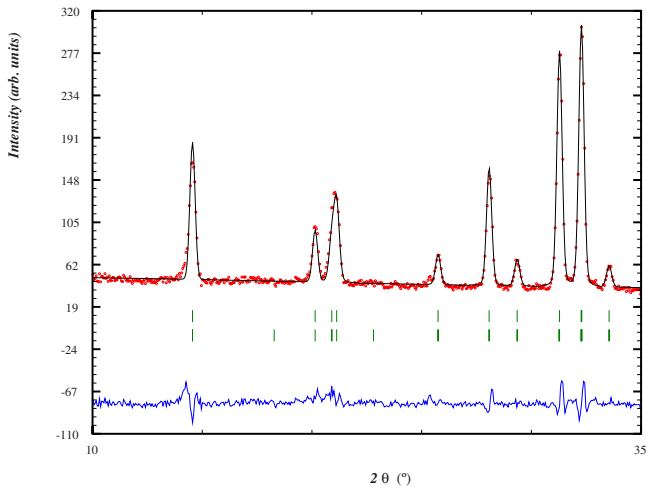

FIG. 10. (Color online) The neutron pattern (λ=1.594 Å) of $NaCrSi_2O_6$ sample collected at 2 K and H=6 T using the D2B diffractometer refined with a ferromagnetic moment $\mu(Cr^{3+})$ =[−1.4(1),0,1.81(7)].

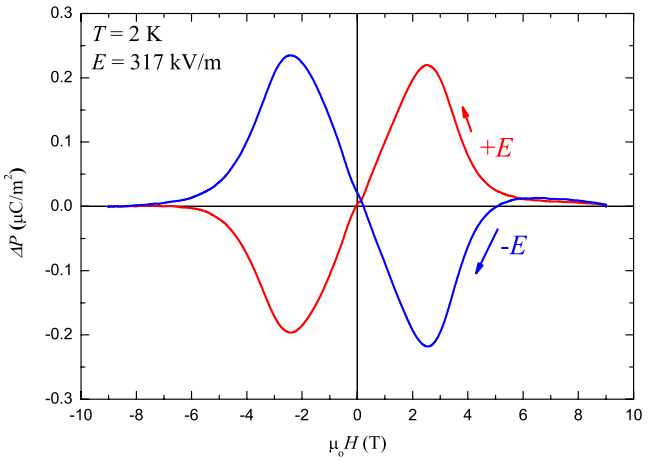

FIG. 12. (Color online) $\Delta P=P-P(9\ \text{T})$ vs H plot obtained after integrating ME current. The ME current was measured in a transverse configuration, i.e., H was perpendicular to E. Magnetic field was varied from −9 to +9 T under applied E. The estimated error on the electrical polarization is about 0.1%.

the magnetoelectric effect decreases and finally vanishes at around 6 T. This can be directly related to our results on the magnetic field dependence of the magnetic structure as determined by neutron diffraction.

While at 1.8 K, a magnetic field of 6 T induces a complete transition from C-1′ toward C2′/c′, this transition is progressive in our polycrystalline sample at intermediate fields. The refinement of the various patterns recorded as function of magnetic field at 1.8 K shows clearly a phase coexistence of the antiferromagnetic and the ferromagnetic phases. This is illustrated in Fig. 13. The phase percentage of the nonmagnetoelectric ferromagnetic phase increases steadily with increasing field and becomes dominant for a magnetic field of 4 T. At 6 T, the antiferromagnetic magnetoelectric phase has completely disappeared. Consequently we can attribute the magnetic field dependence of the electrical polarization as originating from the crossover between the magnetoelectric antiferromagnetic phase to the nonmagnetoelectric ferromagnetic phase which is induced and stabilized under the magnetic field.

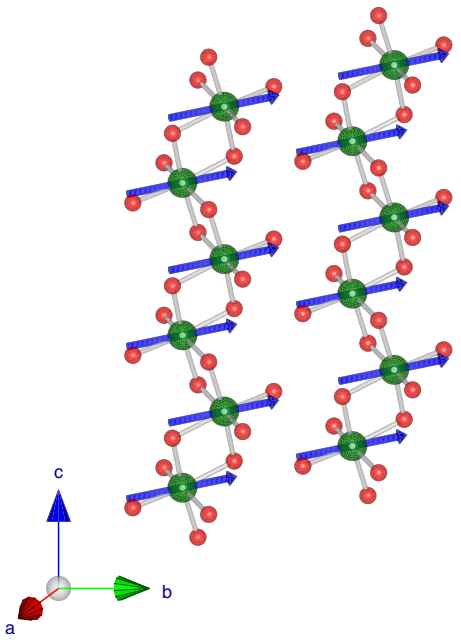

FIG. 11. (Color online) Ferromagnetic structure of $NaCrSi_2O_6$ at 1.8 K and H=6 T described by Γ_3. The magnetic structure representation has been made using VESTA (Ref. 23).

V. DISCUSSION

Neutron powder diffraction experiments confirm that $NaCrSi_2O_6$ exhibits an antiferromagnetic ordering below T_N=2.8(2) K. The magnetic structure is commensurate with the chemical unit cell with $\mathbf{k}$=0 with a magnetic moment of Cr^{3+}=2.31(4)μ_B. The extracted values for J_{intra} and J_{inter} from our SQUID results are confirmed by the magnetic structure determined from neutron diffraction.

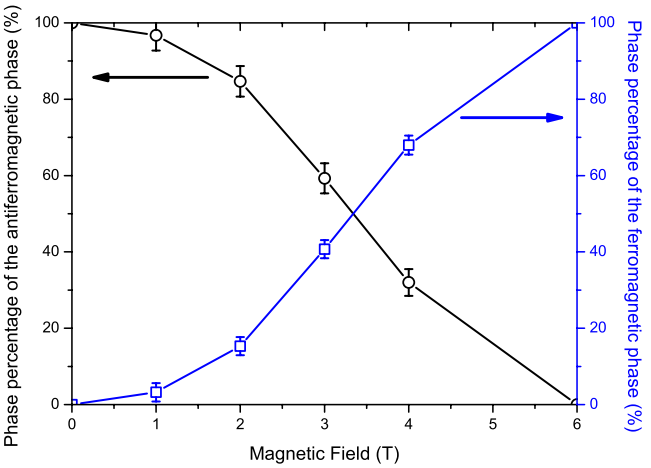

FIG. 13. (Color online) Magnetic field dependence of the antiferromagnetic and ferromagnetic phases expressed in percentage.

The previous estimation of the interchain and intrachain exchange-interaction parameters was made using the relationship between the broad maximum and J_{intra} in half integer $S=\frac{3}{2}$ isolated chains[24] and by using the Schultz formula.[25] It was found that $J_{intra}=J_{inter}=0.8$ K.[18] For a such ratio and value of exchange-interaction parameters, one could expect a spiral spin configuration.[8] However, as seen from our neutron-diffraction data, this is not the case in $NaCrSi_2O_6$. Consequently the model that we use [see Eqs. (1) and (2)] is more appropriate since the determined J_{intra}/J_{inter} ratio is in agreement with the observed commensurate magnetic structure but also gives us the correct sign of the interactions.

In the mean-field approximation, the paramagnetic Curie-Weiss temperature θ is given by[26]

$$\theta = \frac{zS(S+1)}{3}\frac{J}{k_b}, \tag{4}$$

where $S=\frac{3}{2}$ for the spin Cr^{3+}, J is the spin-exchange parameter between two adjacent magnetic sites, and z is the number of nearest-neighbor magnetic sites around a given magnetic site. As an additional consistency check of the determination of J_{intra} and J_{inter} determined using Eq. (2), we compared the paramagnetic Curie temperature θ obtained from the Curie-Weiss fit with the value derived using the values J_{intra} and J_{inter} and Eq. (4).

$$\chi = \frac{C}{T-\theta} = \frac{C}{T-(\theta_{intra}+\theta_{inter})} \tag{5}$$

with $z_{intra}=2$, $z_{inter}=4$, $J_{intra}/k_b=-0.48(4)$ K, and $J_{inter}/k_b=0.24(8)$ K; θ is calculated to be 0.0(3) K according to Eq. (4). This is in excellent agreement with the value −0.22(8) K deduced from the fit of the high-temperature susceptibility (see Sec. III B).

We still have to explain why the found magnetic structure allows for the presence of a linear magnetoelectric effect. We recall that the magnetic space group displayed by $NaCrSi_2O_6$ can be described by the direct product of $\Gamma_2\times\Gamma_4$. In order to determine the magnetic symmetry, one has to consider the common symmetry elements between the two IRs. Looking at Table IV, one notices that there is only one symmetry element in common in both IRs, namely, $-1'$. The centering is not destroyed and thus the magnetic space group is C-1′. The magnetic point group associated to the magnetic symmetry in $NaCrSi_2O_6$ is therefore $-1'$. According to Ref. 13, this magnetic point group allows a linear magnetoelectric effect with the corresponding expression for the tensor

$$\boldsymbol{\alpha_{ij}} = \begin{pmatrix} \alpha_{11} & \alpha_{12} & \alpha_{13} \\ \alpha_{21} & \alpha_{22} & \alpha_{23} \\ \alpha_{31} & \alpha_{32} & \alpha_{33} \end{pmatrix}.$$

We have shown experimentally that this expected magnetoelectric effect is effectively present and its magnetic field dependence in good agreement with our results from neutron diffraction. Applying a magnetic field a ferromagnetic phase is induced resulting in the loss of the magnetoelectric properties at high magnetic field. The magnetic moment at $H=6$ T determined from powder neutron diffraction is $2.62(4)\mu_B$ in good agreement with the magnetization data ($\mu_{sat}=2.56\mu_B$).

We note that the magnetic structure found here for $NaCrSi_2O_6$ is very similar and has the same symmetry as the one reported for $CaMnGe_2O_6$.[11] The difference between these two magnetic structures resides in the magnetic-moment direction which in $NaCrSi_2O_6$ is in the (b,c) plane while it is mostly within the (a,c) plane for $CaMnGe_2O_6$. Consequently, $CaMnGe_2O_6$ is likely to exhibit as well a linear magnetoelectric effect.

VI. CONCLUSION

We have investigated the magnetic and crystal structures of $NaCrSi_2O_6$ as function of temperature and magnetic field using powder neutron diffraction. Below $T_N=2.8(2)$ K, $NaCrSi_2O_6$ exhibits a long-range antiferromagnetic order commensurate with the lattice with $\mathbf{k}=0$. It is characterized by ferromagnetic layers alternating along the c axis giving rise to an overall antiferromagnetic ground state. Using mean-field approximation, we estimated the magnetic exchange-interaction parameters both between and within the chains. We found that $J_{intra}/k_b=-0.48(4)$ K and $J_{inter}/k_b=0.24(8)$ K in good agreement with the magnetic structure determined from neutron diffraction. The associated magnetic symmetry is C-1′. This symmetry allows a linear magnetoelectric effect, which is confirmed experimentally. Application of a magnetic field induces a ferromagnetic phase with the nonmagnetoelectric magnetic symmetry C2′/c′. Additionally, we notice that $NaCrSi_2O_6$ has the same magnetic symmetry as $CaMnGe_2O_6$ and thus the latter is expected to exhibit also a linear magnetoelectric effect. We hope that this study will trigger the investigation of the magnetoelectric properties of other pyroxene materials.

ACKNOWLEDGMENTS

This study is partly supported by a Grant-in Aid for Scientific Research No. 19052008 and RFBR Grant No. 07-02-91201 from the Ministry of Education, Culture, Sports, Science and Technology of Japan and for JSPS (Japan)-RFBR (Russia) Joint Research Project. Work at SNU is supported by the National Creative Research Initiative and KRF (KRF-2008-314-c00101) programs.

*Corresponding author; nenert@ill.eu

[1] M. Fiebig, J. Phys. D **38**, R123 (2005).
[2] W. Eerenstein, N. D. Mathur, and J. F. Scott, Nature (London) **442**, 759 (2006).
[3] S.-W. Cheong and M. Mostovoy, Nat. Mater. **6**, 13 (2007).
[4] A. Pimenov, A. A. Mukhin, V. Yu. Ivanov, V. D. Travkin, A. M. Balbashov, and A. Loidl, Nat. Phys. **2**, 97 (2006); A. B. Sushkov, R. V. Aguilar, S. Park, S.-W. Cheong, and H. D. Drew, Phys. Rev. Lett. **98**, 027202 (2007).
[5] G. Nénert, M. Isobe, C. Ritter, O. Isnard, A. N. Vasiliev, and Y. Ueda, Phys. Rev. B **79**, 064416 (2009).
[6] G. J. Redhammer, G. Roth, W. Treutmann, M. Hoelzel, W. Paulus, G. André, C. Pietzonka, and G. Amthauer, J. Solid State Chem. **182**, 2374 (2009).
[7] S. Jodlauk, P. Becker, J. A. Mydosh, D. I. Khomskii, T. Lorenz, S. V. Streltsov, D. C. Hezel, and L. Bohatý, J. Phys.: Condens. Matter **19**, 432201 (2007).
[8] W.-M. Zhang, W. M. Saslow, and M. Gabay, Phys. Rev. B **44**, 5129 (1991).
[9] M. D. Lumsden, G. E. Granroth, D. Mandrus, S. E. Nagler, J. R. Thompson, J. P. Castellan, and B. D. Gaulin, Phys. Rev. B **62**, R9244 (2000).
[10] G. J. Redhammer, G. Roth, W. Paulus, G. André, W. Lottermoser, G. Amthauer, W. Treutmann, and B. Koppelhuber-Bitschnau, Phys. Chem. Miner. **28**, 337 (2001).
[11] G. J. Redhammer, G. Roth, W. Treutmann, W. Paulus, G. André, C. Pietzonka, and G. Amthauer, J. Solid State Chem. **181**, 3163 (2008).
[12] G. Nénert, C. Ritter, M. Isobe, O. Isnard, A. N. Vasiliev, and Y. Ueda, Phys. Rev. B **80**, 024402 (2009).
[13] International Tables for Crystallography Vol. D, *Physical Properties of Crystals*, edited by A. Authier (Kluwer Academic, Dordrecht, 2003).
[14] J. Rodríguez-Carvajal, Physica B **192**, 55 (1993).
[15] M. Origlieri, R. T. Downs, R. M. Thompson, C. J. S. Pommier, M. B. Denton, and G. E. Harlow, Am. Mineral. **88**, 1025 (2003).
[16] G. J. Redhammer and G. Roth, Z. Kristallogr. **219**, 278 (2004); G. J. Redhammer, G. Roth, and G. Amthauer, Acta Crystallogr., Sect. C: Cryst. Struct. Commun. **64**, i97 (2008); G. J. Redhammer and G. Roth, Z. Kristallogr. **219**, 585 (2004). Please note that the coordinates given in this paper contain an error. The x coordinate of Si_1 is 0.0487 and not 0.487.
[17] G. J. Redhammer, H. Ohashi, and G. Roth, Acta Crystallogr., Sect. B: Struct. Sci. **59**, 730 (2003); C. Satto, P. Millet, and J. Galy, Acta Crystallogr., Sect. C: Cryst. Struct. Commun. **53**, 1727 (1997); E. Baum, W. Treutmann, M. Behruzi, W. Lottermoser, and G. Amthauer, Z. Kristallogr. **183**, 273 (1988).
[18] A. N. Vasiliev, O. L. Ignatchik, A. N. Sokolov, Z. Hiroi, M. Isobe, and Y. Ueda, Phys. Rev. B **72**, 012412 (2005).
[19] J. C. Bonner and M. E. Fisher, Phys. Rev. **135**, A640 (1964); T. Smith and S. A. Friedberg, *ibid.* **176**, 660 (1968).
[20] See, for instance, X.-Y. Wang, H.-Y. Wei, Z.-M. Wang, Z.-D. Chen, and S. Gao, Inorg. Chem. **44**, 572 (2005); E.-Q. Gao, A.-L. Cheng, Y.-X. Xu, M.-Y. He, and C.-H. Yan, *ibid.* **44**, 8822 (2005); K. Shimizu, T. Gotohda, T. Matsushita, N. Wada, W. Fujita, K. Awaga, Y. Saiga, and D. S. Hirashima, Phys. Rev. B **74**, 172413 (2006).
[21] O. V. Kovalev, in *Representations of the Crystallographic Space Groups: Irreducible Representations, Induced Representations and Corepresentations*, edited by H. T. Stokes and D. M. Hatch (Gordon and Breach, Amsterdam, 1993).
[22] Y. A. Izyumov, V. E. Naish, and R. P. Ozerov, *Neutron Diffraction of Magnetic Materials* (Consultants Bureau, New York, 1991).
[23] K. Momma and F. Izumi, J. Appl. Crystallogr. **41**, 653 (2008).
[24] L. J. De Jongh and A. R. Miedema, Adv. Phys. **50**, 947 (2001).
[25] H. J. Schulz, Phys. Rev. Lett. **77**, 2790 (1996).
[26] O. Kahn, *Molecular Magnetism* (VCH Publishers, New York, 1993).